Study of Thermal Characteristics on Solder and Adhesive Bonded Folded Fin Heat Sink

C.K. Loh, Bor-Bin Chou, Dan Nelson and D.J. Chou
Enertron, Inc.
100 West Hoover Suite 5
Mesa, Arizona 85210
(480) 649-5400 FAX: (480) 649-5434
Email: ckloh@enertron-inc.com

ABSTRACT

The rapid advancement in technology of microprocessors has led electronics thermal system designers to pay increased attention to the folded fin heat sink. The advantages of using a folded fin heat sink are light weight, low profile, and small footprint.

There are three manufacturing methods for bonding the folded fin to the base of heat sink: adhesive bonding, soldering, and brazing. Brazing is a high temperature process which takes place at around 550°C. The major concern with using the brazing process to manufacture heat sinks is dimensional deformation. The adhesive process, on the other hand, requires only sub 200°C or room temperature curing process. However, its thermal contact resistance at the joint is higher than others. Solder bonding is an alternative solution to the above problems. The soldering process requires much lower temperature, less than 200°C, yet it gives excellent thermal contact and bond strength at the joint.

This paper presents the theoretical study of thermal contact resistance at the joint between the folded fin base and the spreader plate of heat sink, and also presents the experimental results which support this theory.

KEYWORDS: Solder bonded fin, adhesive bonded fin, bonding thermal resistance, folded fin heat sink, forced convection, air cooled.

NOMENCLATURE

A_{joint}	Area of the joint perpendicular to the direction of heat flux, m^2
h	Convection heat transfer coefficient, W/m^2K
k_{air}	Thermal conductivity of air, W/mK
k_{joint}	Thermal conductivity of the given material, W/mK
k_m	Material thermal conductivity, W/mK
L	Fin Length, m
L_c	Corrected fin length, m
L_{fin}	Length of the fin along the airflow, m
$\overline{Nu}_L$	Average Nusselt number
Pr	Prandtl number
Re_L	Reynolds number
T_{amb}	Ambient Temperature, °C
T_{b_ave}	Average base temperature, °C
T_f	Film temperature, °C
t	Fin thickness, m
t_{joint}	Thickness of the joint in the direction of heat flux, m
U_o	Airflow velocity, m/s
z	Fin width, m
η_f	Fin efficiency
ν	Viscosity of the fluid, m^2/s
Θ_{base}	Heat sink base resistance, °C/W
Θ_{fin}	Resistance from the fin to ambient, °C/W
Θ_i	Interface resistance from the thermoelectric heat pump to the heat sink base, °C/W
Θ_{joint}	Resistance of the joint from the base to the folded fin, °C/W
Θ_{sa}	Overall thermal resistance, °C/W

INTRODUCTION

In the current electronics industry, heat sinks are used extensively to provide cooling for electronics components. The process of making a heat sink is often by extrusion, cold forging, pressed fin, or bonded fins. Even though extruded and cold forged heat sinks require easier manufacturing processes compared to the other two, they have a limited fin aspect ratio due to the manufacturing processes. Whereas the pressed fins or bonded fins techniques offers a higher aspect ratio. Pressed fin is a process where fins are fitted into tapered tip grooves on the base. The fins are pressed by machine to establish contact surface with the base. The disadvantage of this method is that air gaps can exist in the joint which causes higher thermal resistance [1]. However, this problem can be resolved by adding bonding materials, such as adhesive, into the gap.

Both pressed fin methods also require grooves to be made on the base before the bonding process. This method is suitable only for thicker fins. However, the folded fin does not require a grooved base and has no restriction on the fin thickness. This makes folded fins a highly suitable candidate for future electronics in heat rejection. Methods of attaching the folded fin to the base include brazing, adhesive bonding and solder bonding.

Brazing is a process to bond the fins to the base in which molten filler metal fills the surfaces to be joined by capillary attraction in a closed chamber [2]. There are two types of brazing processes, either by aluminum or copper. In aluminum brazing, multiple aluminum sheets having different melting points are clad together and flux is used to remove oxidized deposits from these aluminum surfaces. As this clad

aluminum undergoes high temperature process, the outer aluminum layer with a lower melting point melts and fills the gap between the base and the fins. Copper brazing, on the other hand, uses a forming gas process. In this process, the base and the fins are subjected to nitrogen and hydrogen gas to remove oxidized deposits by forming water through a chemical reaction. The melted brazing material fills the gap between the fin and the base, thus forming the bond. One major drawback in using this process is dimensional deformation when the materials are subjected to high temperatures during the brazing process. Dimensional deformation can alter the geometry of the heat sink.

The second type of bonding is called adhesive bonding. In this process, thin layers of adhesive paste are dispensed on the base. The fins are attached onto the base and the assembly is cured in an oven. In comparison with brazing, adhesive bonding requires a much lower temperature for curing, below 150°C or even room temperature depending on the material [3]. However, thermal resistance along the joint is higher than brazing due to its non-metallic bond and poor thermal conductivity of the adhesive.

The final method of fins to base bonding is soldering. It can be described by dispersion of solder paste to the base through a template called a stencil. The stencil is lifted at the end of the dispersion, and the fins are attached onto the base, ready to be cured. Curing process takes place at a temperature no higher than 200°C. It's Lead-Tin composition gives stronger bonding strength and better thermal contact than epoxy bonded fins because it forms an inter-metallic joint between the solder and the base metal.

This paper compares three different types of bonding processes, silicon based adhesive, heat activated epoxy based adhesive and eutectic solder paste 63Sn/37Pb. The main objective is to determine how the bond effects the thermal performance. It also shows the thermal performance can be effected by varying the thickness and material of the fin.

DESIGN PARAMETERS

The design specifications of a folded fin heat sink found in today's electronics environment are as follows:

- Thickness of folded fin is less than 0.3mm.
- Fin pitch is less than 2.5mm.
- Fin material is either Copper C110 or Aluminum A3003.
- Heat sink base spreader is Aluminum 6063.
- Thickness of base spreader between 5 to 10mm.
- The airflow ranges inside a electronics system ranging from 0.5 to 2.0 m/s, or 100 to 400 fpm.

Test samples are made from the above guidelines that acquired the following conditions:

- Fin Thickness
  ~ 0.2 mm, 0.6 mm and 1.0 mm
- Fin Material
  ~ Copper C110 (k = 380 W/m.°C)
  ~ Aluminum A3003 (k = 180 W/m.°C)
- Base Material
  ~ Copper C110
- Base Thickness
  ~ 2.5 mm
- Bonding Materials
  ~ Lead-Tin solder paste 63Sn/37Pb (k = 39 W/m°C)
  ~ Silicon based adhesive, SE 4420 (k = 1.05 W/m °C)
  ~ Heat activated epoxy, SE 4450 (k = 1.88 W/m°C)
- Experimental Airflow Range
  ~ 1.0 to 3.0 m/s, or 200 to 600 fpm

Based on the above design parameters, a series of single U-shape folded fins experiments has been setup accordingly. The theoretical analysis of the fins are conducted for correlating to the experimental results. Thermocouples are placed under the joint and in the center of fin base for temperature measurement. Figure 1 shows the experimental setup of single U-shape folded fin.

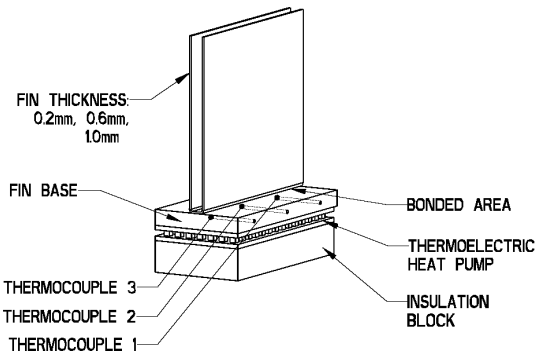

Figure 1. Experimental Setup of Single U-Shape Folded Fin

ANALYSIS METHOD

Theoretical Background

Thermal resistances can be viewed as a circuit joining each other at certain points on the resistance network. In our analysis, the thermal resistance network from heat source to the fins are connected in a series of individual resistances. These individual resistances were then added together to form an overall thermal resistance from base to ambient, $\Theta_{sa,}$ which can be expressed as:

$$\Theta_{sa} = \Theta_i + \Theta_{base} + \Theta_{joint} + \Theta_{fin} \quad (1)$$

With the assumption of no heat lost or gained through the insulator block and since temperatures are measured close to the joint in the base of the heat sink during the experiment, the thermal resistance between the thermoelectric heat pump to the base along with the thermal resistance through the base can be neglected. When these two terms are neglected, the effect of joint thermal resistance will be significantly shown on the overall thermal resistance calculation. Thus, the overall thermal resistance of the system can be re-expressed as:

$$\Theta_{sa} = \Theta_{joint} + \Theta_{fin} \quad (2)$$

Joint Resistance

The joint plays an important role in the heat sink assembly. It forms the bridge that connects the fins and the base together. The temperature of the base partially depends upon the thickness, material type, and contact area of the joint. Increasing the thickness will result in increasing the joint resistance, and increasing the contact area will give the reverse effect. There are many different types of bonding material and their thermal conductivities depend upon their material properties. Typically, the bonding material with higher thermal conductivity will allow greater heat transfer than the one with lower conductivity. The joint area in this analysis is assumed to be the area of the folded fin base that comes in contact with the heat sink base. The joint resistance of the heat sink can be expressed as [4]:

$$\Theta_{joint} = \frac{t_{joint}}{k_{joint} A_{joint}} \quad (3)$$

Fin Resistance

The thermal resistance of the fin, Θ_{fin}, is a function of fin efficiency, η_f , the surface area of the fin, A_f , and the convection heat transfer coefficient, h. Conduction and convection heat transfer are taken into consideration when analyzing the thermal resistance of the fin. Heat is carried through the fin by conduction and dissipated to the surrounding ambient air by convection. The overall resistance of the fin can be written as:

$$\Theta_f = \frac{1}{\eta_f A_f \bar{h}} \quad (4)$$

To evaluate the fin efficiency, first, we must determine the average convection heat-transfer coefficient, $\bar{h}$, where it is given by the expression:

$$\bar{h} = \frac{\overline{Nu_L} k_{air}}{L_{fin}} \quad (5)$$

Based on the assumptions that the fluid properties are constant over the entire fin length, the surface of the fins are assumed to be isothermal, and airflow through the fins are in the laminar regime (Reynolds Number less than 5 x 10^5), the following flat plate empirical approximation can be used to calculate the theoretical average Nusselt Number, $\overline{Nu_L}$ [5] :

$$\overline{Nu_L} = 0.664 \Pr^{1/3} \mathrm{Re}_L^{1/2} \quad (6)$$

The Prandtl Number evaluated at the film temperature, T_f , defined as:

$$T_f = \frac{T_{fin\ surface} + T_{freestream}}{2} \quad (7)$$

Re_L, Reynolds Number is determined by:

$$Re_L = \frac{U_o L}{\nu} \quad (8)$$

Once the Nusselt Number is found using equation (6), the theoretical convection heat transfer coefficient can be determined.

The fin efficiency, η_f, depends on fin thickness, t, material thermal conductivity, k, convection heat transfer coefficient, h, and the corrected length, L_c. To evaluate the fin efficiency, the fin was assumed to have a finite length and the tip of the fin is insulated [6]. With these given conditions, the efficiency of the fin can be expressed as:

$$\eta_f = \frac{\tanh mL_c}{mL_c} \quad (9)$$

and mL_c is given as:

$$mL_c = \sqrt{\frac{h(2z + 2t)}{kzt}} L_c \quad (10)$$

The corrected length, L_c, is defined as

$$L_c = L + \frac{t}{2} \quad (11)$$

with L as the original length of the fin.

When the fin width, $2z$, in the numerator is sufficiently large compared with the fin thickness, $2t$, it can be eliminated from equation (10) and hence, produce the following:

$$mL_c = \sqrt{\frac{2zh}{kzt}} L_c = \sqrt{\frac{2h}{kt}}\ L_c \quad (12)$$

Multiplying the numerator and denominator in equation (12) by $L_c^{1/2}$ gives:

$$mL_c = \sqrt{\frac{2h}{kL_c t}} L_c^{3/2} \quad (13)$$

With $L_c t = A_m$, the profile area of the fin, equation 10 can be expressed as:

$$mL_c = \sqrt{\frac{2h}{kA_m}} L_c^{3/2} \quad (14)$$

With this, the fin efficiency can be determined and after that, the fin resistance can be calculated. Thus, the

overall thermal resistance, Θ_{sa}, in equation (2) can be written as:

$$\Theta_{sa} = \frac{t_{joint}}{k_{joint} A_{joint}} + \frac{1}{\eta_f A_f \bar{h}} \quad (15)$$

THEORETICAL CALCULATION

The theoretical overall thermal resistances are shown on Figures 4, 5, 6, 7, 8 and 9. The thickness effects on thermal resistance are shown on Figures 2 and 3. The thermal resistance decreased by approximately 13% (based on velocity at 3.0m/s) for Copper 110 and 23% (based on velocity at 3.0m/s) for Aluminum 3003 for an increase in fin thickness of 0.2mm to 1.0mm respectively. This is because the larger thickness creates a larger area for heat flux to flow through and thus, reduce the thermal resistance. Also, in comparison between types of bonding, solder bonded fins seem to have 10% (based on 3.0 m/s airflow) better thermal performance over silicon based adhesive bonded fins, and 5% (based on 3.0 m/s airflow) over heat activated epoxy bonded fins for both copper 110 and Al 3003 fins. Assuming there is no contact resistance effect, the lower resistance in the solder bonding is dictated by its thermal conductivity.

Thermal conductivity is a material property. Since solder is a mixture of two metallic materials, whereas, the epoxies are non-metallic in nature, clearly, the solder will have much better thermal performance over the silicon based adhesive and heat activated epoxy.

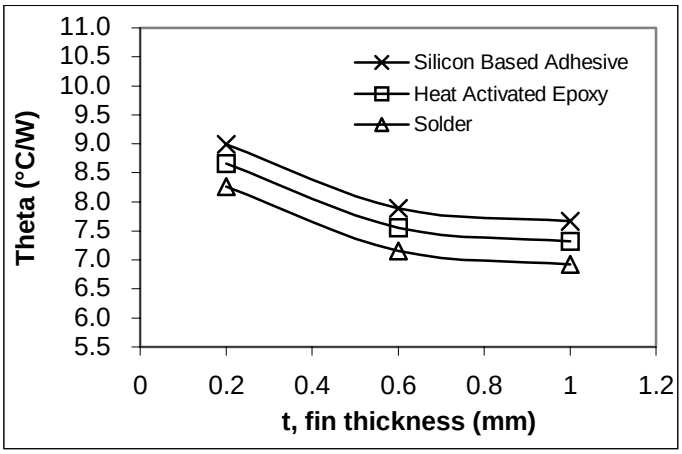

Figure 2. Theoretical Thermal Resistance vs. Fin Thickness at velocity of 3.0m/s for Cu 110 Fin

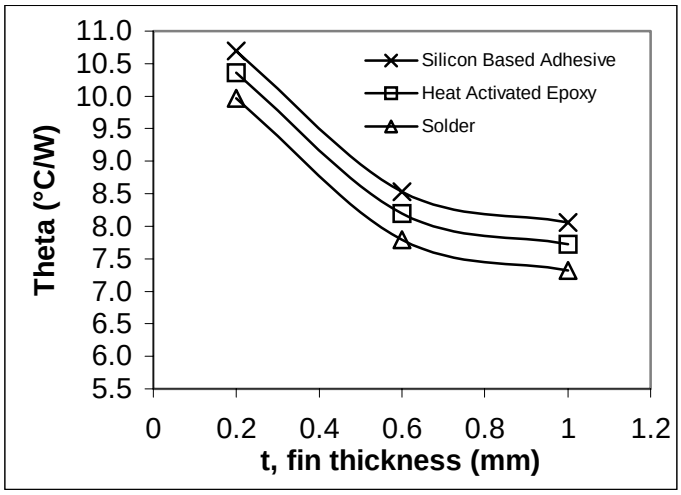

Figure 3. Theoretical Thermal Resistance vs. Fin Thickness at velocity of 3.0m/s for Al 3003 Fin

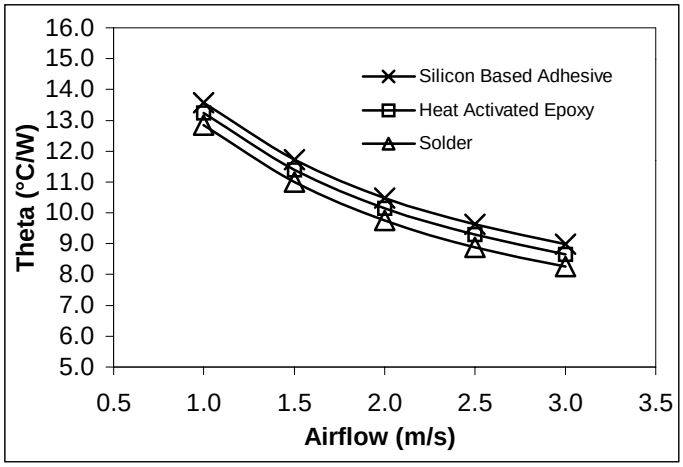

Figure 4. Overall Thermal Resistance (Theoretical) of Bonded 0.2 mm Thick Cu 110 Fin

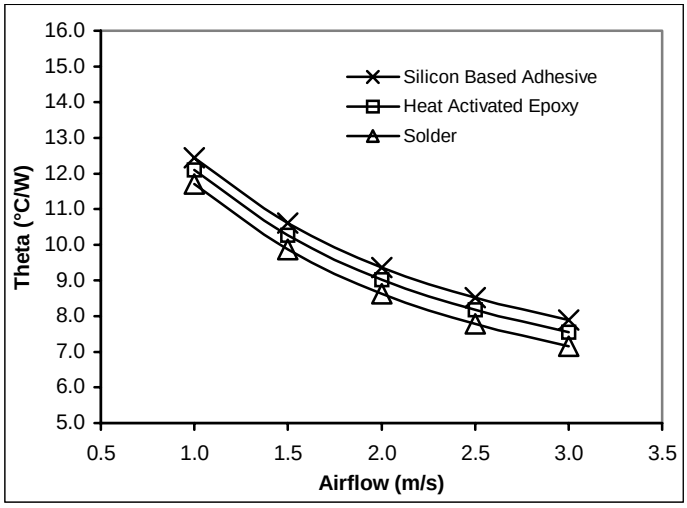

Figure 5. Overall Thermal Resistance (Theoretical) of Bonded 0.6 mm Thick Cu 110 Fin

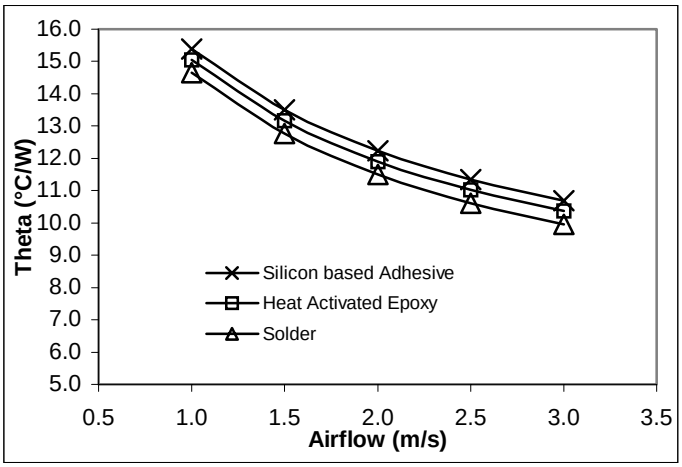

Figure 6. Overall Thermal Resistance (Theoretical) of Bonded 1.0 mm Thick Cu 110 Fin

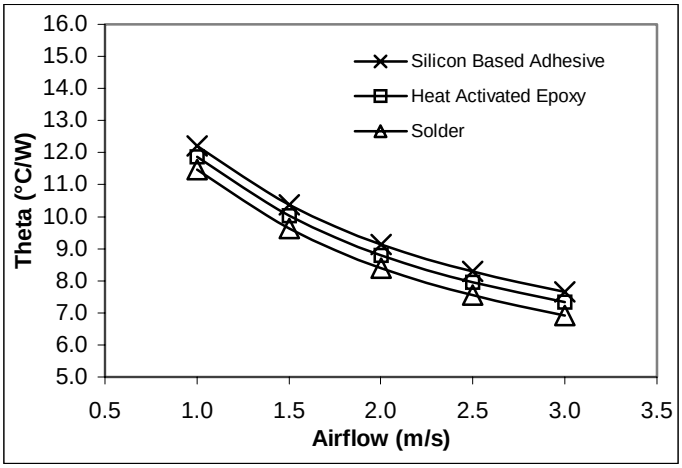

Figure 7. Overall Thermal Resistance (Theoretical) of Bonded 0.2 mm Thick Al 3003 Fin

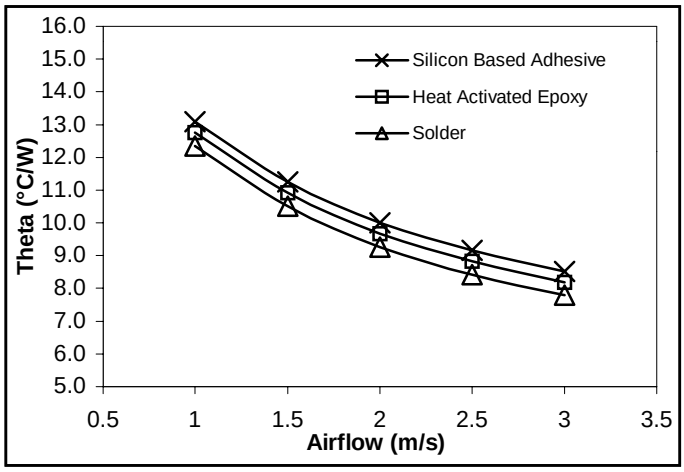

Figure 8. Overall Thermal Resistance (Theoretical) of Bonded 0.6 mm Thick Al 3003 Fin

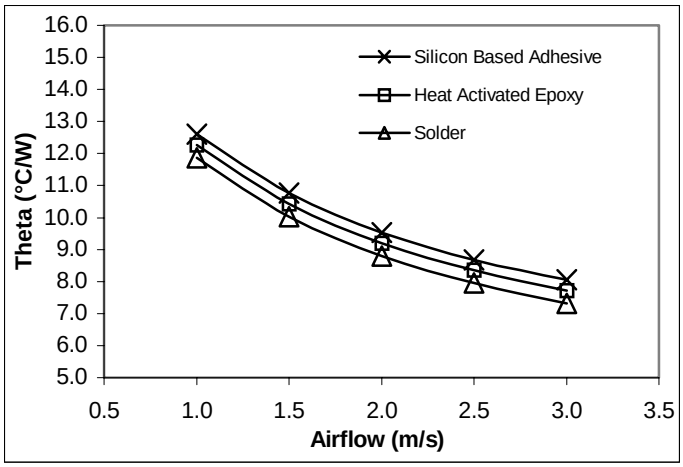

Figure 9. Overall Thermal Resistance (Theoretical) of Bonded 1.0 mm Thick Al 3003 Fin

EXPERIMENTAL PROCEDURE

In the experiment, a Thermoelectric Cooler is used to simulate the heat source. The interface between the TEC and heat sink is covered by a thin layer of thermal grease to eliminate the air gaps which lead to higher thermal resistance. Three thermocouples are placed in the holes of the base for temperature measurement. They are denoted as case temperatures, and one thermocouple is placed outside the test environment for ambient temperature reading.

This test sample is tested inside a bench top wind tunnel shown in Figure 10. The attached blower blows air past the fins and velocity is measured using an anemometer. The experiment begins when the case temperatures of the heat sink are approximately equal to the ambient temperatures. The rise in case temperatures are recorded by a data logger attached to thermocouples at the base of heat sink. Once the case temperatures reach steady temperatures over a period of at least 2 minutes, they are recorded, along with the power supplied to the TEC, and ambient temperature.

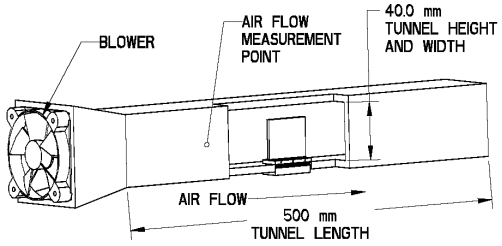

Figure 10. Representation of Bench Top Wind Tunnel

EXPERIMENTAL RESULTS

The experimental thermal resistance, Θ_{sa}, can be evaluated by taking the difference between the average of the base temperature and the ambient temperature divided by the power of the TEC. It can be expressed as:

$$\Theta_{sa} = \frac{T_{b\_ave} - T_{amb}}{TEC\ Power} \quad (16)$$

Once all the thermal resistances, Θ_{sa}, are calculated, they can be plotted against the flow rate to determine the heat sink thermal performance.

The overall thermal performance curves for both Cu 110 and Al 3003 are shown on Figure 13 through Figure 18. The general experimental trends are not as smooth as theoretical trends due to experimental and measurement error. One possible explanation for the deviation lies in the measurement of airflow during the experiment. Airflow varies slightly from one location to another location inside the wind tunnel. Taking measurements at one location inside wind tunnel only measures the velocity of airflow at that particular point. This creates an error in the experimental results because the actual airflow that passes by the fins is not known. In addition, the velocity of airflow that passes through the fins is assumed to be exact in calculating the theoretical thermal resistance, which is not the case in the experimental thermal resistances where these values contain measurement error.

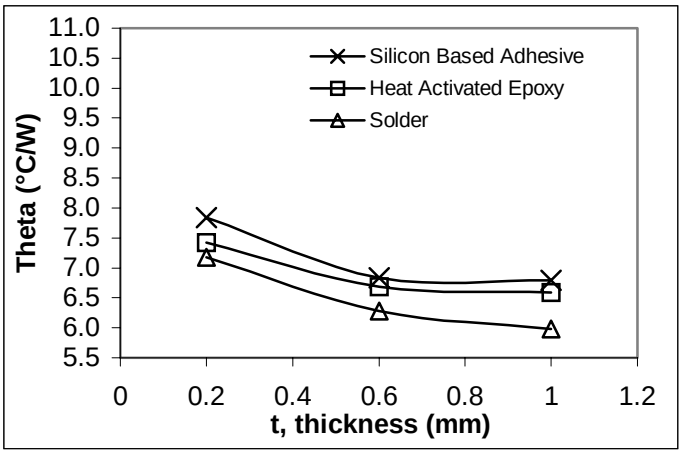

Figure 11. Experimental Thermal Resistance vs. Fin Thickness at velocity of 3.0m/s for Cu 110 Fin

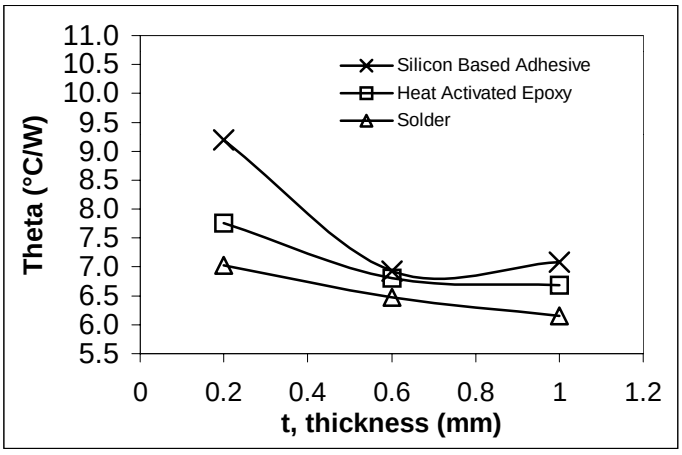

Figure 12 . Experimental Thermal Resistance vs. Fin Thickness at velocity of 3.0m/s for Al 3003 Fin

Figures 13, 14 and 15 show the overall thermal performance of Copper 110 fins. The thermal resistance decreases approximately 12% (Figure 11) as the fin thickness increases from 0.2 mm to 1.00 mm. This seems to agree with the theoretical finding of 13% (based on taking the average of different thickness) for Cu 110. As for the comparison between different types of bonding, the solder 63Sn/37Pb had an average thermal performance of 8% (based on 3.0 m/s airflow) higher than Silicon based epoxy and an average of 5% (based on 3.0 m/s airflow) higher than heat activated epoxy.

The thermal performance curve for Al 3003 are shown on Figure 16, 17 and 18. The solder bonded fins had an average 13% (based on 3.0 m/s airflow) better thermal performance over silicon based adhesive, and 7% better thermal performance over heat activated epoxy respectively (based on 3.0 m/s airflow). There is a 19% (Figure12) increase in thermal performance as thickness of the fins increase. The percentage error for Al 3003 fins, between experimental and theoretical was found to be in the range of 20% to 28% for both cases of different bonded joint and variation in fins thickness.

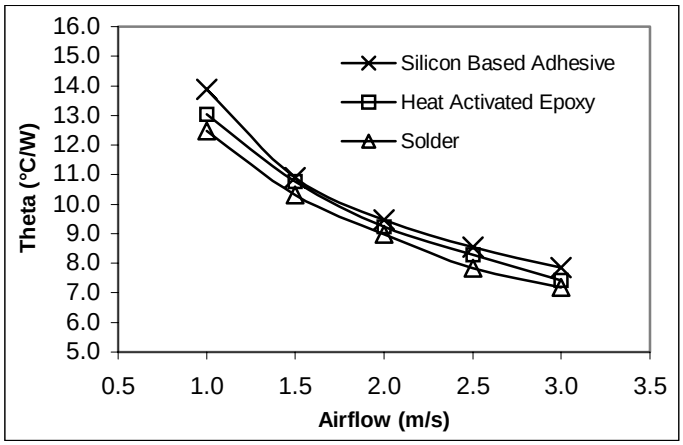

Figure 13. Overall Thermal Resistance (Experimental) of Bonded 0.2 mm Thick Cu 110 Fin

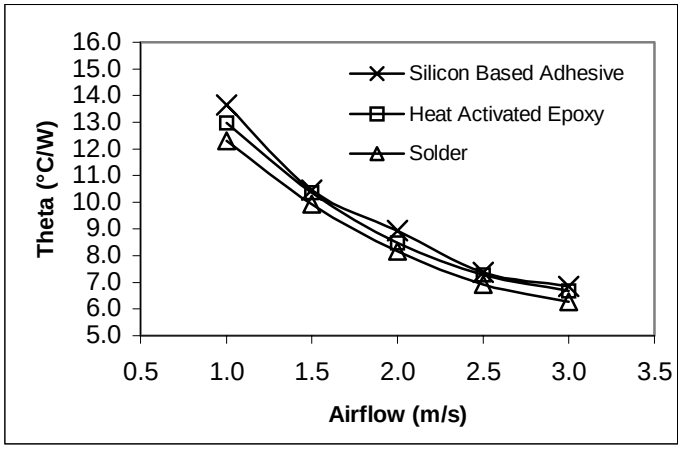

Figure 14. Overall Thermal Resistance (Experimental) of Bonded 0.6mm Thick Cu 110 Fin

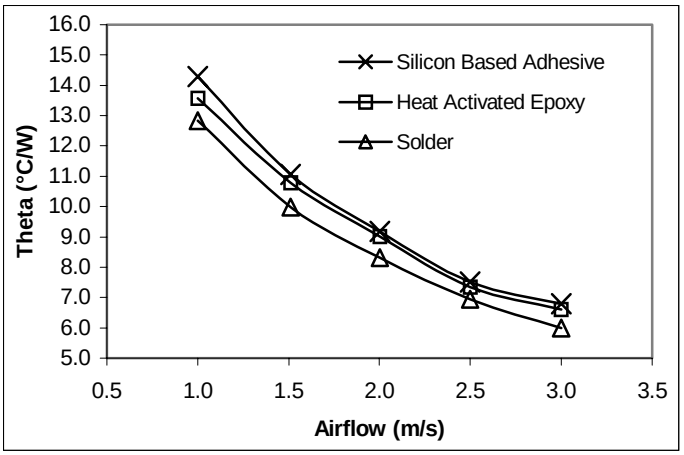

Figure 15. Overall Thermal Resistance (Experimental) of Bonded 1.0 mm Thick Cu 110 Fin

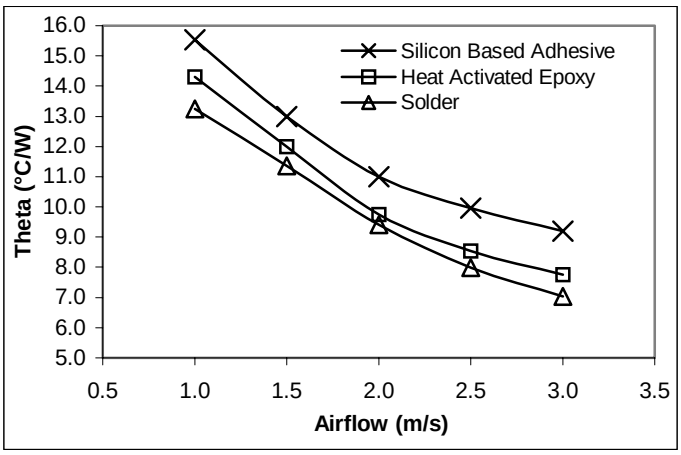

Figure 16. Overall Thermal Resistance (Experimental) of Bonded 0.2 mm Thick Al 3003 Fin

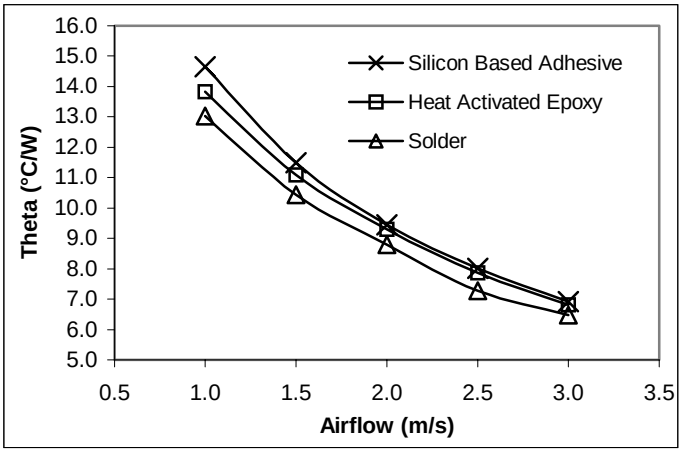

Figure 17. Overall Thermal Resistance (Experimental) of Bonded 0.6 mm Thick Al 3003 Fin

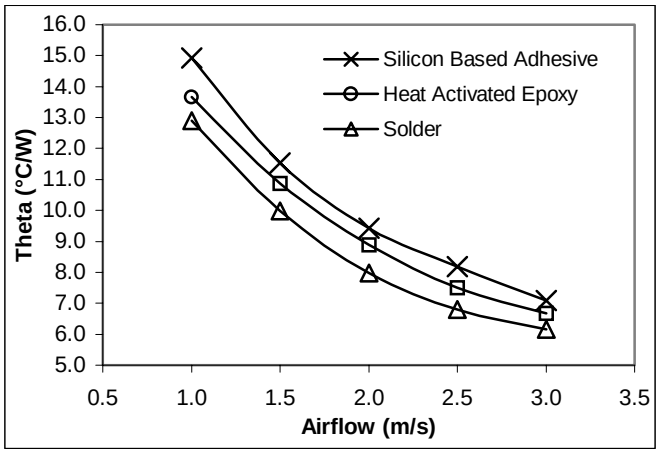

Figure 18. Overall Thermal Resistance (Experimental) of Bonded 1.0 mm Thick Al 3003 Fin

CONCLUSIONS

In summary, the thermal performance of folded fin heat sinks depends on the type of bonded joint, types of material and fin thickness as the theoretical analysis was found to be in agreement with the experimental results. Lower joint thermal resistance for a typical bonded joint folded fin heat sink can be obtained by using solder bonding.

Today, however, the design and selection of heat sinks depend on the nature of its application and cost. There are many factors that effect the performance of the heat sink which must be considered and appropriately selected for optimization.

REFERENCES

[1] E. Fried, Thermal Conduction Contribution to Heat Transfer at Contacts, "Thermal Conductivity," vol. 2, Academic Press, Inc., New York, 1969.

[2] M.D. Jackson, *Welding Methods and Metallurgy*, 1st Edition, Charles Griffin & Company Ltd., London, 1967.

[3] Bryan Ellis, *Chemistry and Technology of Epoxy Resins*, 1st Edition, Blackie Academic & Professional, Glasgow, 1993.

[4] Iuliana M. Bordelon, Jingsong Xie, Yogendra Joshi and Carol Latham, "A Quantitative Assessment of Thermal Interface Materials," Future Circuits International, issue 5, pp 75-78, 1999.

[5] Frank P. Incropera and David P. DeWitt, *Fundamentals of Heat and Mass Transfer*, 4th Edition, Wiley, New York, 1996.

[6] J. P. Holman, *Heat Transfer*, 8th Edition, McGraw-Hill, Inc., New York, 1997.